Exp Brain Res
DOI 10.1007/s00221-007-1009-x

RESEARCH ARTICLE

Deficits of visual motion perception and optokinetic nystagmus after posterior suprasylvian lesions in the ferret (*Mustela putorius furo*)

D. Hupfeld · C. Distler · K.-P. Hoffmann

Received: 15 January 2007 / Accepted: 26 May 2007

Abstract We recently described an area in the ferret posterior suprasylvian (PSS) cortex characterized by a high proportion of direction selective neurons. To answer the question whether area PSS subserves functions similar to cat posteromediolateral suprasylvian area (PMLS) and monkey medial temporal area (MT) we investigated the contribution of area PSS to visual motion perception and optokinetic nystagmus. Ferrets were tested on global motion detection before and after bilateral lesions involving area PSS and control lesions of other extrastriate visual areas. Following PSS lesions motion coherence thresholds were significantly increased both in pigmented and albino ferrets, whereas control lesions sparing PSS did not affect visual motion perception. Optokinetic nystagmus was strongly reduced to absent after PSS lesions. These results indicate that area PSS is crucial for global motion processing in the ferret and in that sense may be functionally equivalent to PMLS in the cat and area MT in the monkey.

Keywords Albinism · Cortical lesion · Motion coherence perception · Optokinetic nystagmus · Posterior suprasylvian cortex

Introduction

A key ability for orienting in a complex visual environment is the perception of visual motion. The basic neuronal substrate for motion perception is presumably direction selective neurons that are especially abundant in extrastriate cortical areas of the dorsal stream, i.e. in the medial temporal (MT) and medial superior temporal area of macaques and probably humans, the posteromediolateral suprasylvian (PMLS) area of the cat, and the posterior suprasylvian (PSS) area of the ferret (ferret: Philipp et al. 2006; cat: e.g. Spear and Baumann 1975; Rauschecker et al. 1987; Sherk 1988; Toyama et al. 1994; Li et al. 2000; Brosseau-Lachaine et al. 2001; monkey: e.g. Maunsell and Van Essen 1983a; Albright et al. 1984; Komatsu and Wurtz 1988; Lagae et al. 1993; man: Nakamura et al. 2003). Indeed, lesions of MT in monkeys and of PMLS in cats produce deficits in global motion perception as well as in optokinetic performance (Strong et al. 1984; Newsome et al. 1985; Duersteler and Wurtz 1988; Newsome and Paré 1988; Tusa et al. 1989; Lomber et al. 1994; Pasternak and Merigan 1994; Rudolph and Pasternak 1996, 1999; Sherk and Fowler 2002). Patients with lesions in area MT (V5) have reduced motion perception (akinetopsia) and are thus severely impaired in everyday life (e.g. Zeki 1991; Schenk and Zihl 1997). Comparable data concerning lesions of ferret area PSS are not yet available.

In recent years, the ferret has become a useful animal model for visual and developmental studies. For comparison with other species it is necessary to explore the extent and function of the various cortical areas in order to draw conclusions about analogous or even homologous areas between species. It has been argued that ferret area 21 may correspond to macaque area V4, that ferret caudal and rostral posterior parietal areas (PPc and PPr, respectively) correspond to primate parietal cortex. Furthermore, area 20a of cat and ferret supposedly corresponds to macaque area TF, area 20b corresponds to TH, and area PS corresponds to TG (von Bonin and Bailey 1947; Payne 1993; Innocenti et al. 2002; Manger et al. 2002a, b, 2004). Based

D. Hupfeld · C. Distler · K.-P. Hoffmann (✉)
Allgemeine Zoologie und Neurobiologie,
Ruhr-Universitaet Bochum, Universitaetsstr. 150,
ND 7/31, 44780 Bochum, Germany
e-mail: kph@neurobiologie.rub.de

on our electrophysiological results and on the retinotopic organization of this area (Cantone et al. 2006), we recently hypothesized that area PSS functionally corresponds to cat PMLS and monkey MT (Philipp et al. 2006). Preliminary anatomical results strengthen this assumption because area PSS, similar to PMLS and MT, projects to the key subcortical structures involved in the generation of eye movements, i.e. the pons, the nucleus of the optic tract and dorsal terminal nucleus (NOT-DTN), lateral and medial terminal nucleus of the accessory optic system, as well as the superior colliculus (cat: e.g. Kawamura et al. 1974; Berson and Graybiel 1980; Marcotte and Updyke 1982; monkey: e.g. Maunsell and Van Essen 1983b; Standage and Benevento 1983; Ungerleider et al. 1984; Distler et al. 2002; ferret: Distler et al. 2006).

Furthermore, the ferret is the only carnivore with readily available albinotic strains and thus offers the opportunity to study the effects of albinism in a mammal with a higher developed cortical visual system than rodents and lagomorphs. Albinism is caused by mutations in the tyrosine metabolism leading to very characteristic anatomical and physiological alterations especially in the visual system (for review see Jeffery 1997). Typically, albino mammals including humans show a highly variable and often severely disturbed optokinetic reaction (Hahnenberger 1977; Collewijn et al. 1978, 1985; Demer and Zee 1984; St John et al. 1984; Abadi and Pascal 1994). In albino ferrets, a regular optokinetic reaction cannot be elicited at all, probably due to the lack of direction selective neurons in the NOT–DTN of these animals (Hoffmann et al. 2004). One possible explanation for this loss of direction selectivity could lie in the nature of the cortical projections from area PSS to the NOT–DTN, i.e. the corticofugal projection neurons could lack direction selectivity, they could code for other than ipsiversive stimulus movement, or they could suppress the ipsiversive response of their target neurons in the NOT–DTN.

The direction selectivity in albino ferret PSS is impaired when compared to wildtype ferrets (Philipp et al. 2006). We recently proposed that this reduced direction selectivity in albino PSS may reflect the neuronal basis for the impaired but not missing ability of albino ferrets to detect global motion (Hupfeld et al. 2006). Therefore, albino ferrets were included in this study to investigate whether bilateral lesions of area PSS might further impair or even destroy their residual motion sensitivity, or alternatively lead to a disclosure of a subcortical optokinetic performance by removing a potentially suppressive input to the NOT–DTN.

In the present study the discrimination performance for global motion was investigated before and after lesions involving area PSS or control lesions involving areas 19 and/or 18 in eight ferrets. The hypothesis to be tested was that motion perception should mainly involve dorsal stream area PSS whereas motion perception should be little affected by control lesions not involving PSS.

Materials and methods

Animals

A total of eight adult ferrets, two albino and two wildtype females, two albino and two wildtype males, participated in the present experiments. These animals had also partaken in a recent study of motion perception (Hupfeld et al. 2006). Ferrets were bred and raised in the animal facility of the Department of General Zoology and Neurobiology, Ruhr-University Bochum, except for one wildtype male which was purchased from Marshall Farms, North Rose NY, USA. Animals were between 3 and 5 years old at the beginning of the experiments, males were fertile whereas female ferrets were castrated. Individuals were marked by a subcutaneous passive transponder chip. Ferrets were group-housed in an enriched environment with access to an outdoor enclosure. Animals were food deprived and received their daily ration as reward during the experiments. Body weight was monitored daily before the test session. At any one time, two ferrets of the same sex and phenotype were trained and tested parallel to each other and were lesioned on the same day, one receiving bilateral lesions involving area PSS and the other receiving control lesions (CTRL) of other visual cortical areas. Cases are labelled by type of lesion (PSS, CTRL), the phenotype (wt, a), and a number corresponding to the size of the lesion (1 representing the smallest, 4 the largest one) (Table 1). Albino females case PSSa-1 and case CTRLa-2 were tested parallel to each other as were wildtype females case PSSwt-2 and case CTRLwt-1, albino males case PSSa-3 and case CTRLa-3, and wildtype males case PSSwt-4 and case CTRLwt-4. The experiments were performed in accordance with the European Communities Council Directive of 24 November 1986 (S6 609 EEC), as well as the National Institutes of Health guidelines for the care and use of animals for experimental procedures. Experiments were approved by the local authorities (Regierungspräsidium Arnsberg) and were carried out in accordance with the Deutsche Tierschutzgesetz of 12 April 2001.

Discrimination setup and procedure

The setup for assessing visual discrimination ability using a two alternative forced choice paradigm was a modified discrimination box (Fig. 1a). The setup and the test procedures were described in detail recently (Hupfeld et al. 2006). In short, both stimuli were presented on one monitor next to each other to create a “left” versus “right” choice situation.

Table 1 Summary of areas affected by lesions

Case	Sex	Hemisphere	Areas involved	White matter involved
PSSa-1	F	Left	PSS, 21, 19, (18)	++
		Right	PSS, 21, 19, 18 v, 17 v	++
PSSwt-2	F	Left	PSS, 21, parietal	+
		Right	PSS, 21, (19), parietal	+
PSSa-3	M	Left	PSS, 21, 19 v, 18 v, parietal	++
		Right	PSS, 21, 19, 18, 17, parietal	++
PSSwt-4	M	Left	PSS, 21, auditory, parietal, (temporal)	+++
		Right	PSS, 21, (auditory) (parietal)	+++
CTRLwt-1	F	Left	19 d, 18 d, (17)	+
		Right	19 d, 18 d	+
CTRLa-2	F	Left	19, 18	+
		Right	19, 18, (17)	+
CTRLa-3	M	Left	18, 17	++
		Right	18, 17, (19)	++
CTRLwt-4	M	Left	19, 18, 17	++
		Right	19, 18, (17)	+++

For each case the areas affected in both hemispheres are listed with the animal's sex, the phenotype is indicated by the case name. Areas which were only partly affected are shown in brackets. The number of + signs qualitatively indicates the amount of underlying white matter involved in the lesion

17 area 17, *18* area 18, *19* area 19, *21* area 21, *auditory* primary auditory cortex, *a* albino, *d* dorsal part of the area affected, *F* female, *M* male, *PSS* posterior suprasylvian cortex, *v* ventral part of the area was affected, *wt* wildtype

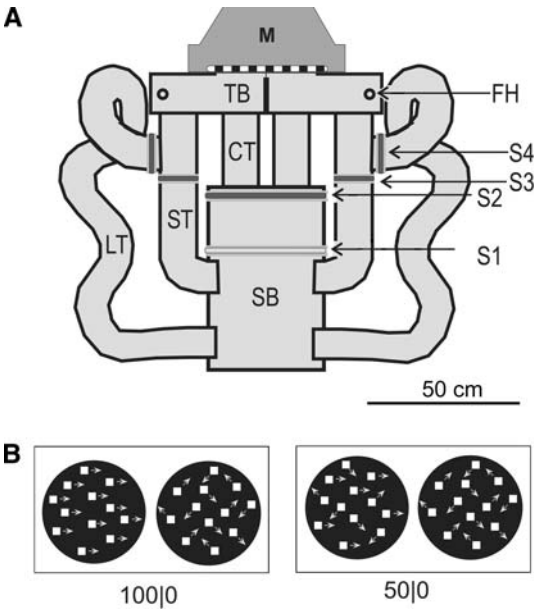

Fig. 1 **a** Experimental setup as seen from above. *CT* choice tube, *FH* food hole, *LT* long tube, *M* monitor, *S1* transparent slide, *S2* opaque slide, *S3* slide 3, regulating access to ST, *S4* slide 4, regulating access to LT, *SB* start box, *ST* short tube, *TB* target box. A ferret in *SB* can see the stimuli on the monitor if *S2* is lifted. Lifting *S1* allows access to both *CT*. A choice is indicated by entering the *left* or *right CT*. Food reward is given via *FH* in the *top* of the *TB*s. For detailed procedures see Sect. "Materials and methods". *Scale bar* represents 50 cm. **b** Illustration of motion coherence stimuli as seen through choice tubes. Level 100|0, 100% coherence versus a dynamic noise (0% coherence), is shown in the *left panel*. The *right panel* shows 50% coherence versus noise (S+ in the *left window*)

Two parallel horizontal tubes were arranged in front of the monitor leading from the centre box towards the stimuli. The operant behaviour consisted of passing through one of these choice tubes. A transparent slide in front of the choice tubes was used to prevent the animal from entering unless a minimal presentation time of 1 s had passed. Movable slides were also used to guide the ferret through the setup for each trial, i.e. slides were lifted in front of the ferret and lowered immediately after the passage of the animal. A correct choice was rewarded by food, a false choice was punished by a prolonged way back to the central box. The apparatus was cleaned after each session. Olfactory or auditory clues from the food reward can be excluded because, first, across the session correct choices were distributed evenly between left and right, and second, because the reward was dropped into the food hole only after the animal had indicated its choice by entering the choice tube (Fig. 1a). To reduce the influence of the experimentor there was no direct contact with the ferret during the experiment and the setup was covered by dark materials. The animals received the remainder of their daily ration after the session in a separate box, water was available ad libitum in their home ranges.

Stimuli

Moving random dot patterns of adjustable coherence were created and presented with the software "randomdots" developed by B. Krekelberg. The patterns consisted of randomly distributed white dots (squares) on a black background. Apparent motion of the dots was created by shifting their position between single frames. The lifetime

of each dot was limited to 1 s after which it vanished and was replaced at a random new position. The proportion of dots moving in the same direction (i.e. to the right) is referred to as the percentage of motion coherence, an incoherent motion is created by equal proportions of dots moving in different directions (dynamic noise). At the decision line (entrance to the choice tubes) the visible stimulus area was 12° of visual angle in diameter for each choice alternative. Stimulus velocity was 10°/s, dots were 1°× 1° of visual angle in size with a mean dot density of 0.5/deg^2. The chosen stimulus velocity proved to be effective in driving neurons in area PSS as well as in areas 17 and 18 (Baker et al. 1998; Moore et al. 2005; Philipp et al. 2006). The same stimulus velocity was used for all tests before and after the lesions.

As a basic visual detection task a white (W) field was presented as the rewarded (S+) versus a blank (B) screen as the non-rewarded (S−) stimulus. This level will be referred to as W|B. Level 100|B, a 100% coherently moving random dot pattern versus a blank screen, was used to re-establish choice of the coherent pattern (S+) even though at this level discrimination could be based on luminance. Pre-lesion motion coherence thresholds for each ferret participating in this study were obtained during previous experiments (Hupfeld et al. 2006). Patterns of different coherence (100, 75, 50, 25, and 5%; but not each level for each animal) versus dynamic noise (0% coherence) were used to test motion perception before and after lesions (Fig. 1b). Two ferrets were trained and tested with levels between 100 and 5% coherence, all other ferrets were just retrained for the present experiments to re-establish performance. After the lesions ferrets were tested with a limited set of coherence values. Females were tested with levels down to 50% coherence which was close to their detection threshold. Thus, an increase in the coherence threshold would result in a decrease of performance at least at this level. Males PSSwt-4 and CTRLwt-4 were additionally tested with another set of stimuli including 100 and 75% coherence.

As a control two male ferrets were further tested in an additional stationary grating discrimination task with vertical square wave gratings as rewarded (S+) stimuli presented versus noise patterns (each dot position had a 50% chance as being assigned as black or white (100% noise) (S−). Gratings had a spatial frequency of 0.5 cycles per degree visual angle (six full cycles) and consisted of 60 × 60 squares (0.2° × 0.2° v.a.) which were either black or white (100% coherence). Gratings of different coherence (100, 50, 33, and 17%) had to be discriminated from choice alternatives of the same mean luminance but built from randomly distributed black and white squares. That means that in the 33% coherence grating 33% of the dots in the black bar were assigned black and 33% of the dots in the white bar were assigned white. The other dots had a 50% chance of being either black or white (Nguyen et al. 2004).

Training schedule

All animals had previously partaken in experiments investigating motion perception thresholds (Hupfeld et al. 2006). As there was a time lapse of several months between the former and the present experiments, several weeks of pre-lesion retraining (at least 20 sessions) were conducted to ensure stable performance. The method of constant stimuli was used to measure discrimination performance for different degrees of coherence. A set of four fixed stimulus coherence levels was used within one session, for example 100, 75, and 50% coherence (versus 0%) as well as a control stimulus as W|B. Levels changed from trial to trial in a randomized order, resulting in about ten non-consecutive repetitions for each of the four levels used within one session. The sets were changed between sessions to test different levels, e.g. the lower coherence levels in cases PSSa-3 and CTRLa-3 (Fig. 2). Each session thus produced results for four levels, mean performance for each level was finally calculated over multiple sessions. From the resulting psychometric function of discrimination performance (% correct choices) versus different stimulus intensities (% motion coherence) the post-lesion coherence threshold was evaluated as the stimulus intensity at criterion performance. Already a few hours after the surgery all ferrets were able to walk, eat and behave normally. Thus, behavioural tests could continue one or 2 days after surgery. For the first 3 days after surgery ferrets received full food rations even if they performed only a few trials or performed at low accuracy (evaluated for the easiest level). Sessions were abandoned in case of disturbance behaviour which could be interpreted as sign of discomfort of the animal. After about 5 days of training a 2-day break was allowed as additional recovery time.

In the first four animals the location of the lesion was known to the experimentor during the post-lesion tests. Experiments in the four remaining ferrets were done in a

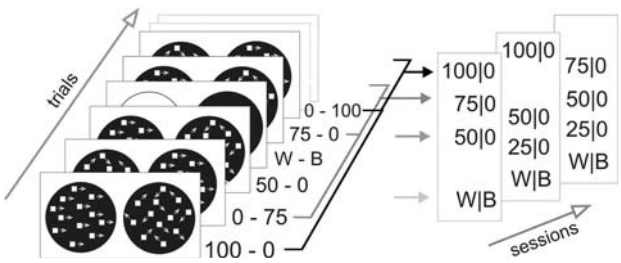

Fig. 2 Cartoon demonstrating the method of constant stimuli used in the present investigation. The *numbers* indicate coherence levels. For further explanation see text

double blind manner. In the 4–6 weeks of post-lesion survival time 20–25 test sessions (with about 20–50 trials each) were performed thus approximately reaching the number of sessions before surgery.

Horizontal optokinetic responses

Optokinetic responses were measured by electro-oculography (EOG) before and after surgery. For eye movement recordings ferrets were sitting snugly in a plastic tube, head movements were restrained by a harness. Fine (100 µm diameter) varnish-coated Ag/AgCl electrodes were inserted subcutaneously at the temporal canthus of each eye after local anaesthesia with lidocaine hydrochloride (Xylocain® 2%, Astra Zeneca). Ferrets were then placed in the centre of a drum covered with a black and white Julesz pattern (dot size 10° contrast 87%, mean luminance about 15 cd/m^2. The drum rotated in clockwise (cw) or counterclockwise (ccw) direction at a speed of 10°, 20° and 50°/s for optokinetic stimulation. Conjugate eye movements in the horizontal plane were measured as differential signal between both eyes. EOG signals were amplified and recorded with a temporal resolution of 100 Hz over 30 s for different stimulus conditions. The signal was not calibrated, thus only a relative value for eye velocity (as mV potential) was obtained. The method and the differences between albino and wild-type ferrets was presented in detail in a recent study in which the males of the present investigation also participated (Hoffmann et al. 2004). Female ferrets were either tested with EOG or by video observation of optokinetic behaviour prior to the lesions. One or two post-lesion EOG measurements during binocular (and monocular for wild-type ferrets) vision lasting up to 1.5 h were performed about 2 weeks after surgery. Monocular measurements for both eyes often had to be done in different sessions. In each session at least three recordings per stimulus velocity and direction were performed per viewing condition.

Surgery

After premedication with 0.05 mg/kg atropine sulphate i.m. (Atropinsulfat Braun® 0.5 mg/ml) ferrets were initially anaesthetized with 20 mg/kg ketamine hydrochloride and 2 mg/kg xylazine (Rompun® 2%) i.m.. The animals were intubated through the mouth after local anaesthesia with lidocaine (Xylocain® Astra Zeneca, 10 mg/100 mg), and a catheter was introduced into the cephalic vein. After additional local anaesthesia with bupivacaine s.c. (bupivacaine-hydrochloride-monohydrate; Bupivacain-RPF® Aventis, 5 mg/ml) the animals were placed into the stereotaxic frame, the skin overlying the skull was cut, and the temporalis muscle was deflected to expose the surface of the skull. Bilateral craniotomies were performed at stereotaxic coordinates anterior 3 to posterior 7, lateral 4 to lateral 12 to allow access to extrastriate visual cortex.

The cortical targets were identified by visual inspection of the sulcal pattern, especially the lateral and suprasylvian sulci as depicted in Fig. 2 (Fox 1998; Manger et al. 2002a). Then a small opening was made in the overlying dura, and the relevant cortical grey matter was removed by aspiration via a 1 mm wide needle. After completion of the lesions, the treated areas were covered with gelfoam (Braun). Then the bone flaps were replaced, the temporalis muscle reflected, the wound sutured in appropriate layers, and covered with antibiotical ointment (Nebacetin® Yamanouchi).

During the whole procedure, animals were artificially ventilated with air containing 0.8–1.0% halothane as needed (Ugo Basile rabbit ventilator, 25–30 ml/stroke, 28–33 strokes/min). Body temperature, heart rate, and endtidal CO_2 were monitored continuously and maintained at physiological levels. In addition, animals received a continuous intravenous infusion of electrolytes and 5% glucose (Sterofundin® B. Braun, Glucose 5 B. Braun as 2:1; at 4 ml/h). To prevent edema, 2 ml mannitol (10% Mannit, Braun) were administered intravenously prior to the lesions. In addition, animals received prednisolone (Predixon®, Chassot, 0.1 ml/kg) i.m. to prevent inflammation. After full recovery, the animals were returned to their home enclosure. Animals were treated with analgesics (Carprofen, 2.5 mg/kg, Rimadyl® Pfizer) s.c. for 2 days and broadband antibiotics (enrofloxacin, 5% Baytril® Bayer) s.c. for 1 week after surgery.

Histology

To evaluate the position and dimension of lesions, ferrets were sacrificed about 4–6 weeks post-lesion. After an overdose of pentobarbital (Narcoren®) administered intravenously the animals were perfused transcardially with 0.9% NaCl, followed by 4% paraformaldehyde. After cryoprotection with 10, 20, and 30% sucrose the brains were shockfrozen in isopentane at −70°C after having been photographed. Frontal sections were cut at 50 µm thickness on a cryostat and adjacent sections were stained for cytoarchitecture (Nissl), Klüver–Barrera, and myeloarchitecture (Gallyas 1979; as modified by Hess and Merker 1983).

For evaluation of the size and position of the lesions the cresyl violet stained sections were drawn using a microscope (Zeiss Axioscop) with camera lucida. The borders of the lesioned area as well as the lips of sulci were marked and used for surface reconstructions of the lateral view of the cortical hemispheres to allow comparison of the lesioned areas. As cyto- and myeloarchitecture could not be unequivocally interpreted close to the lesioned regions areal borders were implied from data from the literature in these cases (Innocenti et al. 2002; Manger et al. 2002a, b, 2004; see Fig. 2, inset).

Data analysis

Analysis of discrimination performance consisted of calculating the percentage of correct responses for each session and the mean values over all sessions for each stimulus level. If less than ten trials at one level were obtained within a session data were pooled for this and the following session for this level. Motion coherence thresholds were estimated from the resulting psychometric functions. The mid-value between guess (50% correct choices for 0% coherence) and lapse rate (best performance, usually close to 90% correct choices) of each individual was taken as threshold criterion, which was close to 70% correct choices. This individualized criterion was established for these experiments in the previous study (Hupfeld et al. 2006) because female ferrets showed a lower average best performance than males. Thus, a fixed criterion would have underestimated the coherence thresholds in females. For males the resulting criteria were close to 70% correct choices, for females criteria were about 67% correct choices due to their lower best performance. The effects of lesions were analysed by comparing pre- and post-lesion performance of each individual separately. For statistical analysis a non-parametric Mann–Whitney and a paired *t*-test were used. If the probability of an error in rejecting the hypothesis that the two paired samples did not differ was below 5%, the null-hypothesis was rejected and the difference between pre- and post-lesion performance was regarded as significant ($P < 0.05$). The immediate effect of the lesions on performance was additionally investigated by comparing the performance of the last sessions before and the first sessions immediately after the lesion (two to three sessions to obtain about 20 trials per level).

For the analysis of EOG data, recording sequences without disturbances due to minimal head and body movements were selected and the median inclination of the signal was calculated. This slope corresponds to the relative eye velocity during the OKN slow phase. Symmetry of OKN was judged by comparing relative eye velocity during cw and ccw stimulation in the same session. Optokinetic responses were also analysed qualitatively with respect to regular OKN eye movements observed before and after lesions, or to any irregularity (strong monocular asymmetry, spontaneous nystagmus, lack of responses), respectively.

Results

Reconstruction of cortical lesions

Table 1 summarizes the location of cortical lesions performed in the individual animals. For comparison, size and location of all lesions are demonstrated on the reconstructed lateral views of all cortical hemispheres in Figs. 3 and 4. To facilitate the appreciation of the ferret's

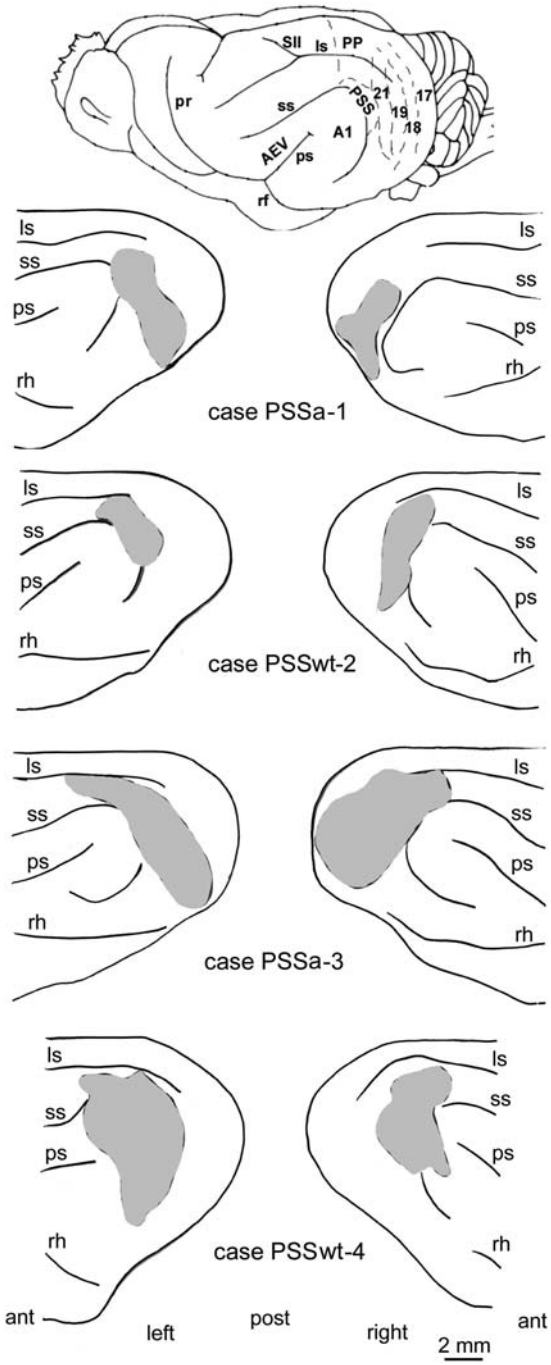

Fig. 3 Reconstructions of the lateral views of all cases with PSS lesions. The schematic view of the *left hemisphere* depicted in the *top panel* supplies the relative position and extent of various cortical areas. Regarding the lesions, case PSSa-1 (*top*) represents the smallest, case PSSwt-4 the largest lesions. The posterior pole of each lesioned hemisphere is shown in the *middle* of the figure, the anterior part of the cortex points to the *left* (*left hemisphere*) or to the *right* (*right hemisphere*), respectively. The *shaded regions* indicate the lesioned areas. *ls* lateral sulcus, *pr* presylvian sulcus, *ps* pseudosylvian sulcus, *ss* suprasylvian sulcus, *rh* rhinal fissure, *A1* primary auditory cortex, *AEV* anterior ectosylvian visual area, *PP* posterior parietal areas, *PSS* posterior suprasylvian visual area, *SII* secondary somatosensory area; areas 17, 18, 19, 21. The *scale bar* represents 2 mm

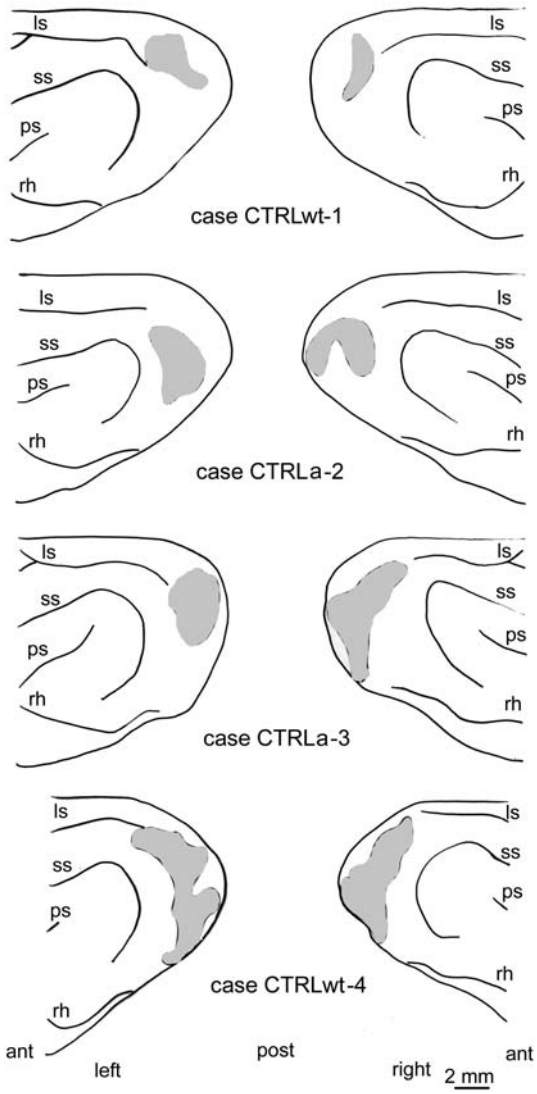

Fig. 4 Reconstructions of the lateral views of all cases with control lesions (*CTRL*). Conventions as in Fig. 3. *Scale bar* represents 2 mm

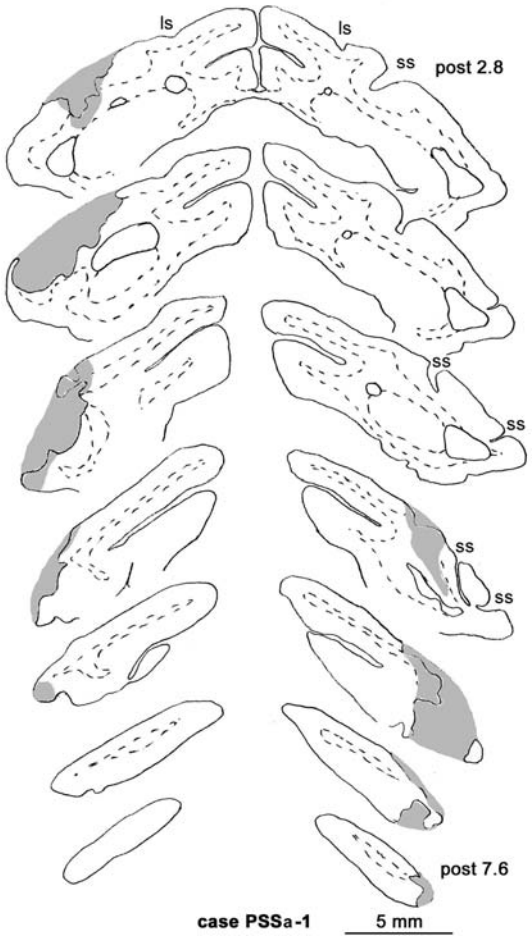

Fig. 5 Reconstruction of frontal sections through the cortex of case PSSa-1 showing the smallest of our PSS lesions. The sections are 800 µm apart and arranged from posterior (*bottom*) to anterior (*top*). *Dashed lines* indicate the border between *grey* and *white matter*, *grey areas* indicate the missing or damaged tissue. The lesioned region in this case spans the cortex from posterior 7.6 to posterior 2.8. For abbreviations see Fig. 3. *Scale bar* indicates 5 mm

various visual areas the top panel in Fig. 3 schematically shows the approximate location and extent of these areas based on our own data and data taken from the literature (Innocenti et al. 2002; Manger et al. 2002a, b, 2004; Cantone et al. 2006; Philipp et al. 2006). Our lesions show some variability both in the exact location and in overall size. Nevertheless, all PSS lesions (shaded areas in Fig. 3) involved area PSS as well as neighbouring areas, whereas all control (CTRL) lesions (shaded areas in Fig. 4) involved more posterior visual areas but spared area PSS.

For the sake of brevity we only demonstrate serial sections of the smallest and the largest lesion of each type to visualize the extent of the damage. Figure 5 shows serial sections through the cortical hemispheres of case PSSa-1. The lesions include the posterior part of the suprasylvian cortex comprising area PSS, as well as area 21, parts of area 19, and ventral regions of area 18. Figure 6 presents the serial sections through the brain of case PSSwt-4. These rather large lesions encompass the whole extent of area PSS and area 21 in addition to parts of the auditory, parietal, and temporal cortex. In this case, the underlying white matter was compromised over most of the extent of the lesions. Especially in the left hemisphere, the cerebral ventricle was significantly enlarged.

All control lesions spared area PSS by a wide margin (Fig. 4). The most restricted lesions are represented by case CTRLwt-1 (Fig. 7). In both hemispheres the lesions cover the dorsal parts of area 19 and 18 with some possible involvement of area 17 in the left hemisphere. As shown by the sections in Fig. 7 the underlying white matter is mostly spared in this case. The much larger lesions in case

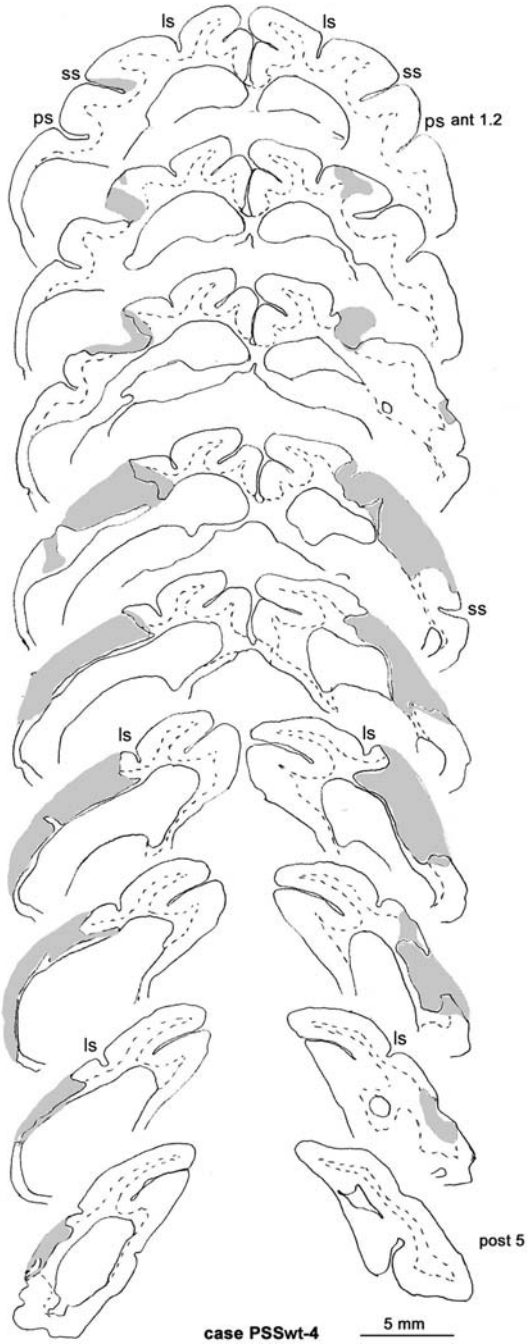

Fig. 6 Reconstruction of frontal sections through the brain of case PSSwt-4 showing the largest of our PSS lesions. Conventions as in Fig. 5. Note the extensive damage of the underlying *white matter* and the enlarged ventricles especially in the *left hemisphere*. The lesion in this case spans the region between posterior 5.0 and anterior 1.2

CTRLwt-4 (Fig. 8) include large parts of areas 19, 18, and 17 with considerable involvement of the white matter. In all lesions, the involvement of the white matter was restricted to the lesioned areas as judged by inspecting neighbouring sections stained for different protocols.

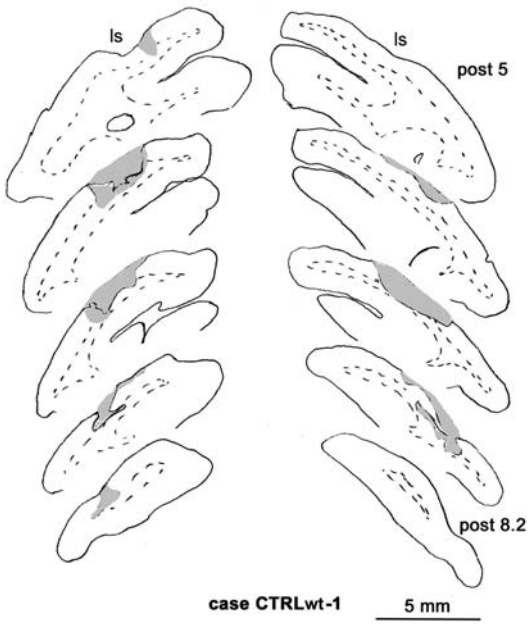

Fig. 7 Reconstruction of frontal sections through the cortex of case CTRLwt-1 showing the smallest of our control lesions. Conventions as in Fig. 5. The lesion in this case spans the region between posterior 8.2 and posterior 5.0

Pre- and post-lesion visual motion discrimination performance

There was only a short break of 2–3 days between the pre- and post-lesion test period. In order to demonstrate the degree of individual variability data from all ferrets were analysed and compared separately.

Visual discrimination performance based on luminance differences (W|B: a white versus a blank field; 100|B: a random dot pattern of 100% coherence versus a blank screen; 100|S a random dot pattern of 100% coherence versus a stationary random dot pattern) was not impaired by the lesions in any of the PSS or CTRL cases ($P > 0.05$, paired t-test; Fig. 9a–h).

The immediate effects of lesions on motion detection, i.e. the performance of the first post-lesion sessions amounting to a minimum of 20 trials per level, were comparable to the overall effects during the whole post-lesion survival period. In no case did we see any indication for recovery of function. Thus, Fig. 9 shows for all ferrets the average performance during 4 weeks before and after the lesion. There was an immediate post-lesion decrease of discrimination performance in females with PSS lesions by 5–40% correct choices, which reduced performance of PSSwt-2 for all coherence levels and for PSSa-1 for all except 100% coherence to chance level (Fig. 9a, b). Reliable discrimination between dynamic noise and coherently moving patterns with less than 100% coherence was not

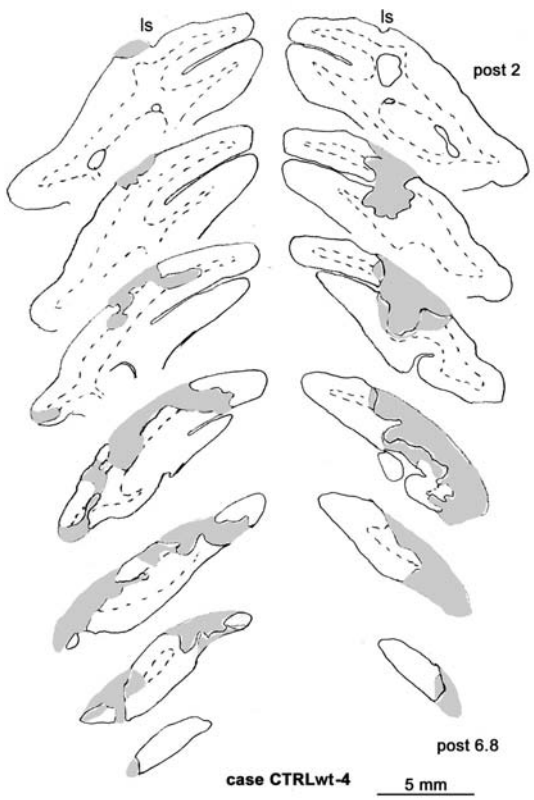

Fig. 8 Reconstruction of frontal sections through the brain of case CTRLwt-4 showing the largest of our control lesions. Conventions as in Fig. 5. The lesion in this case spans the region between posterior 6.8 and posterior 2.0. Also in this case there is extensive damage to the underlying *white matter*

achieved immediately after lesions nor during the whole test period (Fig. 9a, b) in these animals. As performance did not recover even after retraining sessions on the full coherence level, post-lesion motion coherence thresholds could not be calculated for cases PSSa-1 and PSSwt-2 (Table 2).

Male ferrets with PSS lesions showed a decrease of discrimination performance in the motion coherence test of about 10–40% correct choices (Fig. 9c, d). The resulting motion coherence thresholds showed an increase by 63% coherence for PSSa-3 and by 77% coherence for PSSwt-4 (Table 2). To gain sufficient data points before and after lesion in view of the rather large variability of the behavioural responses for statistical analysis we pooled all motion coherence levels tested in the individual animals. In each ferret with bilateral lesions involving PSS, performance was significantly reduced after lesion (range of *P*-values for Mann–Whitney tests of individual ferrets 0.002–0.03; range of *P*-values for individual *t*-tests 0.001–0.016).

Ferrets with control lesions (females CTRLwt-1, CTRLa-2 and males CTRLa-3, CTRLwt-4) showed no such difference between pre- and post-lesion performance in the motion coherence task (Fig. 9e–h; Mann–Whitney $P = 0.42 - 0.78$; *t*-test $P = 0.07 - 0.96$). The *P*-values of the Mann–Whitney tests for the comparison of pre- and post-lesion performance are indicated for the individual animals in Fig. 9a–h. Although motion detection performance was slightly lower immediately after the lesion in these animals the difference was well within the range of normal variability. There were only slight changes in motion coherence thresholds in CTRLwt-1 and CTRLa-2, i.e. a slight decrease of threshold was observed in CTRLwt-1 and an increase in CTRLa-2, both within a range of 5% coherence (Table 2).

A slightly increased motion coherence threshold of 4% was observed after lesion in albino male CTRLa-3, in wildtype male CTRLwt-4 the post-lesion threshold was not assessed for all coherence levels. For the few levels tested the results corresponded to those of case CTRLa-3 (Table 2).

Thus, while CTRL lesioned animals were only slightly, if at all, impaired in motion coherence detection all PSS lesioned ferrets showed severe impairment or even a complete lack of motion coherence detection. Importantly, as long as area PSS was removed the severeness of the impairment in motion coherence detection did not depend on the size of the lesion or the amount of damage to the white matter. The lesion effects were comparable in individuals of both phenotypes.

The post-lesion performance in the pattern coherence detection task remained nearly constant in case PSSa-3 but not in wildtype ferret PSSwt-4. Unexpectedly, this animal showed an increase of the pattern coherence threshold by 30% possibly due to the massive involvement of the underlying white matter. Thus, even though this animal had a significant deficit in motion coherence detection it can not serve as a valid support for the significant role of area PSS for motion detection because of its obvious deficits also in pattern discrimination. In view of the large extent of the lesion, the involvement of the underlying white matter, and the enlarged ventricles seen in this animal (Fig. 6) we can not exclude the possibility of damage to the optic radiation in this case. Pattern discrimination deficits were not present in the other PSS lesioned animal (Fig. 10) which had the second largest lesion. Thus, in this and supposedly the other two animals with even smaller PSS lesions PSS seems to be the critical structure for coherent motion detection.

Horizontal optokinetic reaction

Head nystagmus or abnormal body postures were not observed in any of the animals after PSS- or CTRL-lesions. The comparison of pre- and post-lesion performance of ferrets with control lesions revealed no change in optokinetic performance. Generally, optokinetic behaviour of the two wildtype ferrets corresponded to data in the literature (Hein et al. 1990; Hoffmann et al. 2004). There was a correlation

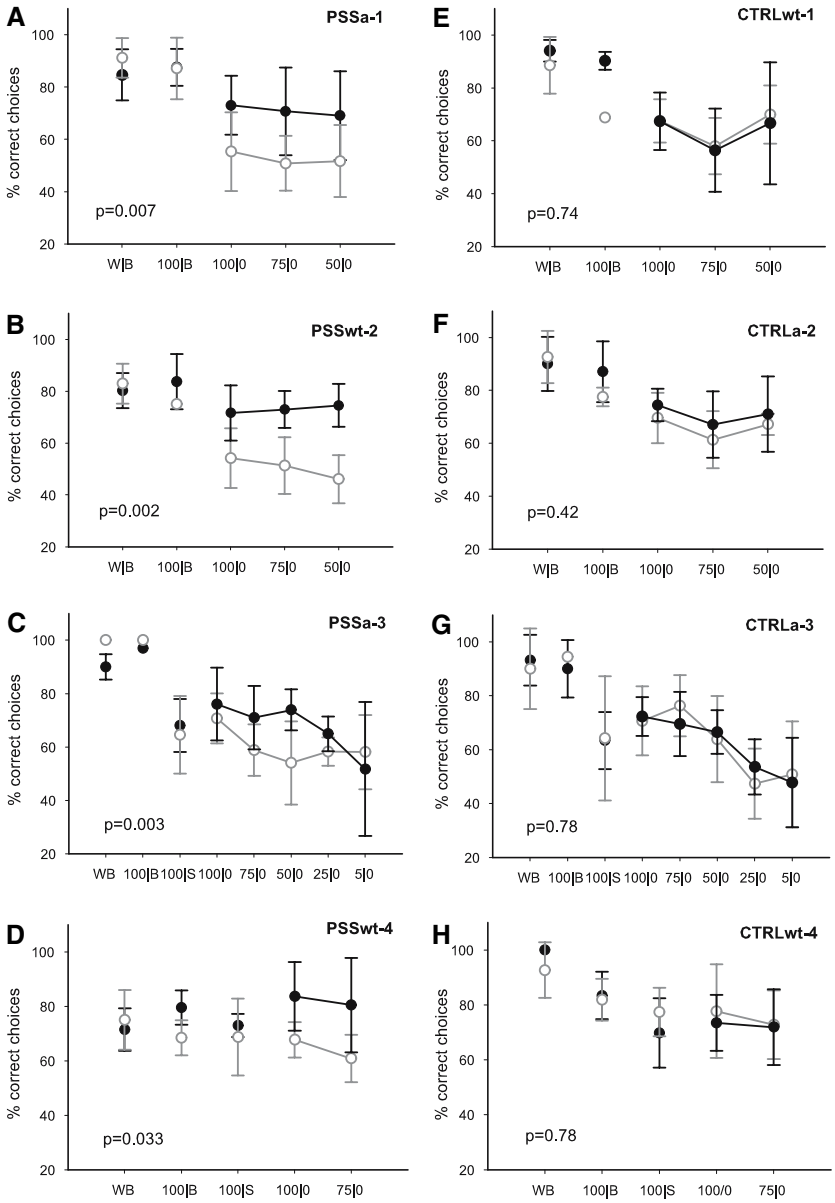

Fig. 9 Motion coherence detection performance of ferrets before (*black lines*) and after the lesions (*grey lines*). *Filled black dots* and *open grey circles* indicate the mean performance before and after the lesion, respectively. *Vertical bars* indicate one standard deviation. The *P*-values given in the *individual plots* indicate the statistical difference (Mann–Whitney rank sum test) between pre- and post-lesion performance of each animal averaged over all coherence levels tested in this individual. *Ordinate* percentage of correct choices, *abscissa* percentage of coherence of the rewarded stimulus. **a** albino female PSSa-1, **b** wildtype female PSSwt-2, **c** albino male PSSa-3, **d** wildtype male PSSwt-4, **e** wildtype female CTRLwt-1, **f** albino female CTRLa-2, **g** albino male CTRLa-3, **h** wildtype male CTRLwt-4. For cases PSSwt-4 and CTRLwt-4 the 50% coherence level was not tested repeatedly

between relative eye velocity and stimulus velocity, i.e. relative eye velocity increased with stimulus velocity (Table 3). After the lesion relative eye velocity during binocular viewing was slightly lower than before the lesions (case CTRLwt-1) or unchanged (case CTRLwt-4).

Monocular responses were nearly symmetrical, i.e. the ferrets responded about equally well to stimulation in temporo-nasal and naso-temporal direction. If responses were not equal they had a higher gain in temporo-nasal direction.

Lesions of area PSS had variable effects on optokinetic performance in the two wildtype ferrets. Post-lesion optokinetic responses were elicited equally well in both directions in wildtype female PSSwt-2 under binocular viewing conditions but declined at higher stimulus velocities. However, during monocular viewing this ferret showed only weak optokinetic responses both for temporo-nasal and naso-temporal directions. In addition, a spontaneous nystagmus with the slow phases directed to the right was occasionally observed. The post-lesion optokinetic behaviour of wildtype male PSSwt-4 showed severe deficits with a spontaneous nystagmus towards the left under binocular viewing, a weak response with a leftward nystagmus for monocular right and irregular responses for monocular left stimulation.

The albino ferrets (PSSa-1, PSSa-3, CTRLa-2, CTRLa-3) participating in this experiment showed the phenotype specific optokinetic deficit, i.e. no optokinetic responses could be elicited before and after the lesions. In addition, no spontaneous nystagmus was observed after cortical lesion. Thus, the cortical lesions did not obliterate any putative

Table 2 Motion coherence thresholds

Cases	Pre (%)	Post (%)
PSS		
PSSa-1	43	ND
PSSwt-2	24	ND
PSSa-3	32	95
PSSwt-4	20	97
CTRL		
CTRLwt-1	38	33
CTRLa-2	47	50
CTRLa-3	46	50
CTRLwt-4	18	16

Summary of motion coherence thresholds before (pre) and after (post) cortical lesions

*ND*threshold could not be determined because even a stimulus of 100% coherence was not detected above chance level

suppressive cortical influence upon the subcortical substrate of the optokinetic reflex.

Discussion

In the present study we investigated the contribution of motion sensitive area PSS to global motion perception by comparing the performance before and after cortical (PSS) lesions. The lesions applied in the present experiments were of variable size and not limited to single areas (Table 1). However, there is a clear distinction between the two lesion types: PSS lesions always included PSS, control lesions always excluded this area.

Lesion effects on motion coherence discrimination

The global motion detection ability of all ferrets with PSS lesions was decreased if not completely absent independent of their gender or phenotype. By contrast, lesions involving parts of area 17, 18, and 19 but sparing area PSS had no or only insignificant effects on global motion detection even though at least area 18 also contains motion sensitive cells and has recently been shown in cats to respond to pattern motion signals (Schmidt et al. 2006). Interestingly, motion perception deficits were reported in human patients with a small lesion in area V2 (area 18) (Vaina et al. 2000) and in parieto-occipital cortex (Blanke et al. 2003).

The impaired motion coherence detection after PSS lesion is comparable to the consequences of PMLS lesions in cat and MT lesions in monkeys (Newsome and Paré 1988; Pasternak and Merigan 1994; Rudolph and Pasternak 1996). Similarly to our results, coherence thresholds of cats were increased from about 25 to 75% coherence after lesions of lateral suprasylvian areas (Huxlin and Pasternak 2004). When measuring within the affected visual field, coherence thresholds of about 8–10% coherence were increased to 10–20% coherence after MT lesions in macaque monkeys (Rudolph and Pasternak 1999).

We performed the pre- and post-lesion tests with the same set of stimuli and at the same stimulus velocity. Thus, we cannot exclude that the animals would have been able to perform global motion detection at different combinations of spatial and temporal frequencies in the motion display. Indeed, data from human patients indicate that for example spatial summation may influence the magnitude of motion detection deficits and recovery of function (Beardsley and Vaina 2006), and that different cortical regions are specialized for different aspects of motion perception (Vaina et al. 2005; see also Palmer and Rosa 2006).

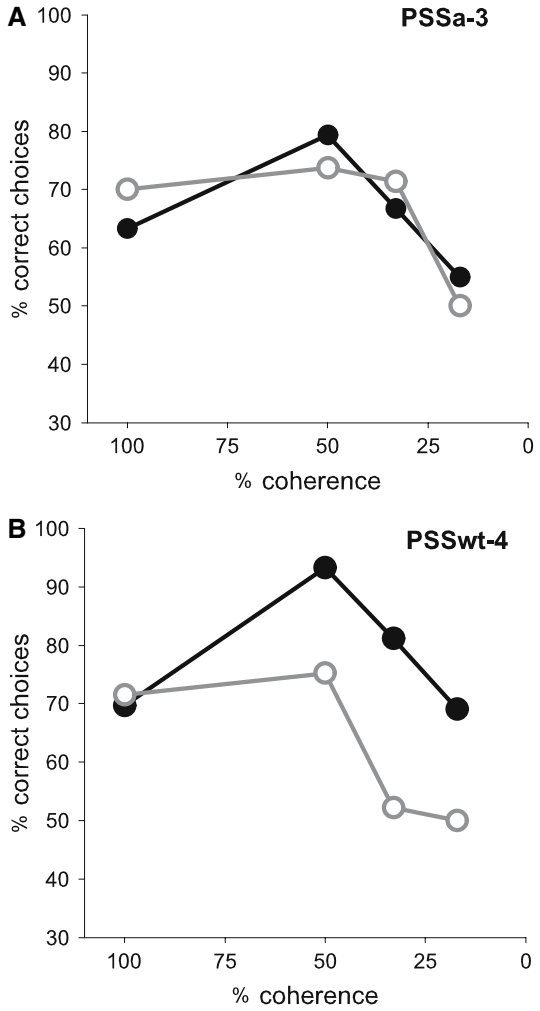

Fig. 10 Pattern coherence detection performance of male ferrets PSSa-3 (**a**) and PSSwt-4 (**b**) during the last pre-lesion (*black lines*, *solid symbols*) and first post-lesion sessions (*grey lines*, *open symbols*) (based on about 20 trials per level). *Ordinate* percentage of correct choices, *abscissa* percentage of coherence of the rewarded stimulus

Table 3 Lesion effects on relative eye velocity during binocular horizontal optokinetic nystagmus

Case	Type	Sex	Pre-lesion			Post-lesion performance		
			10°/s	20°/s	50°/s	10°/s	20°/s	50°/s
PSSwt-2	WT	F	Regular OKN, observed by video	Regular OKN, observed by video	Regular OKN, observed by video	0.05 mV/s	0.12 mV/s	0.05 mV/s
PSSwt-4	WT	M	0.53 mV/s	0.56 mV/s	–	0.20 mV/s	0.05 mV/s	0.1 mV/s
CTRLwt-1	WT	F	0.11 mV/s	0.21 mV/s	0.32 mV/s	0.06 mV/s	0.12 mV/s	0.15 mV/s
CTRLwt-4	WT	M	0.06 mV/s	0.25 mV/s	0.49 mV/s	0.20 mV/s	0.30 mV/s	0.60 mV/s
PSSa-1	ALB	F	No OKN	No OKN	No OKN	No OKN	No OKN	No OKN
PSSa-3	ALB	M	No OKN	No OKN	No OKN	No OKN	No OKN	No OKN
CTRLa-2	ALB	F	No OKN	No OKN	No OKN	No OKN	No OKN	No OKN
CTRLa-3	ALB	M	No OKN	No OKN	No OKN	No OKN	No OKN	No OKN

Lesion effects on optokinetic performance

Eye movement recordings were performed in order to judge qualitatively if wildtype animals developed optokinetic pathologies after the lesions, i.e. spontaneous nystagmus, marked asymmetries of monocular optokinetic nystagmus or even loss of this reflex. As the EOG measurements were not calibrated we made no attempt to quantitatively compare eye movement accuracy, i.e. gain, before and after the lesion. There is strong evidence from the literature that the quality of OKN in higher mammals crucially depends on the presence and functional properties of the cortical input to the NOT–DTN. Indeed, PSS lesions in ferrets led to ocular instabilities in the wildtype animals PSSwt-2 and PSSwt-4. Spontaneous nystagmus occurred during monocular viewing in case PSSwt-2 and during binocular and monocular viewing in case PSSwt-4. Head nystagmus or abnormal body postures were not observed in any of the animals. No obvious effect on optokinetic behaviour was seen after control lesions. This clearly indicates that ferret area PSS is involved in the cortical control of the optokinetic system.

We have shown earlier that albino ferrets lack optokinetic eye movements, that the characteristic direction selectivity of retinal slip cells in the NOT–DTN is missing, and that area PSS is less direction selective in albinos than in wildtype ferrets (Hoffmann et al. 2004; Philipp et al. 2006). As area PSS projects to the NOT–DTN (Distler et al. 2006) we also tested with the present experiments the hypothesis that in albinos the cortical input from area PSS to the NOT–DTN in some way obscures or hampers direction selectivity in the NOT–DTN neurons, e.g. by transmitting directional signals not in accordance with the ipsiversive preference of the NOT–DTN neurons or by suppressing the retinal slip neurons in the NOT–DTN. The resulting loss of direction selectivity would render the NOT–DTN unable to trigger OKN.

However, there was no disclosure effect of PSS or control lesions on optokinetic performance in albino ferrets, i.e. albino ferrets were unable to perform regular OKN before and after cortical lesions independent of their location. Furthermore, no spontaneous nystagmus was observed after lesion. Thus, our present results suggest that the lack of direction selectivity in the NOT–DTN and the inability to perform optokinetic reactions in albino ferrets is not caused by an abnormal cortical input from area PSS. These results are an important step towards clarifiying oculomotor pathologies in albino mammals.

Recovery of function after lesions

Previous work has shown that motion perception can recover after lesions. However, this recovery of function needs extensive specific training (Huxlin and Pasternak 2004). In the present study, a survival time of 4–6 weeks was allowed. During this period a recovery of motion perception was not observed in any of the four animals with PSS lesions. Also for ferrets with control lesions, which had only mild effects on their motion coherence performance, no improvement was observed throughout the post-lesion test period.

In most studies reporting functional recovery ibotenic acid lesions were applied whereas in our study the cortical gray matter was actually removed. Also training intensity was considerably less in our study. In cats with lesions of the lateral suprasylvian sulcus recovery of motion perception occurred after 2–7 weeks of extensive training consisting of a total of 1,000–2,700 trials (Huxlin and Pasternak 2004). In our study only about 200–570 post-lesion trials were performed in the motion coherence detection task. In macaques, recovery of motion perception after MT lesions clearly depended on the kind of stimulus used despite of extensive training (Rudolph and Pasternak 1999).

Location and size effects of lesions

Comparing the size of the individual lesions with the resulting behavioural defects it becomes clear that the deficits in motion detection are evidently correlated with the location but not the size of the lesion. Even if we discount case PSSwt-4 because of its additional defects in stationary pattern coherence discrimination the reduction in motion perception ability in case PSSa-3 was similar to that found in cases PSSa-1 and PSSwt-2 which had much smaller lesions. Deficits in motion perception were not observed after control lesions. Additionally, optokinetic behaviour was affected after PSS lesions in wildtype animals but not after control lesions of other extrastriate areas. This clearly indicates that the deficits found in our study are not the non-specific consequence of traumatic brain injury but are due to the ablation of a specific area, in our case PSS. Similar results can be found in the literature where lesion of specific areas as PMLS or MT lead to very specific deficits in oculomotor behaviour and motion perception but not in other tasks (e.g. Lynch and McLaren 1983; Spear et al. 1983; Ventre 1985; Tusa et al. 1989; Lauwers et al. 2000; Blanke et al. 2003). Lesions of V1 on the other hand produce no such deficits (e.g. Ventre 1985; Pasternak et al. 1995; Guo et al. 1998). In a differentiated series of tests, sensitivity for drifting gratings at low spatial frequencies and direction discrimination was unaffected by V1 lesion, the performance in a global motion detection task was even better after V1 lesion (Pasternak et al. 1995). Given the similar anatomical position of MT, PMLS, and PSS on the respective cerebral hemispheres and the similar deficits reported after lesions made with ibotenic acid or by physical ablation we deem it unlikely that the observed PSS-lesion effects were due to damage of the anterior white matter and optic radiation. The question remains why no significant motion detection deficits were evident after lesions of the primary visual areas, i.e. the putatively main cortical input structures for area PSS. First, areas 17, 18, and 19 were not removed in total. Thus, the remaining parts could provide sufficient driving input to area PSS. Second, preliminary anatomical data indicate that area PSS is reciprocally connected with the pulvinar and, to a lesser degree, with the dorsal lateral geniculate nucleus (Distler et al. 2006). Therefore, visual information can reach area PSS via this secondary visual pathway. To which degree this secondary connection plays a significant role in the intact system remains unclear at this point.

The cortical white matter in our cases was affected to a varying degree. Generally, white matter damage was largely restricted to the site where the grey matter was removed. Due to the tangential approach of the aspiration needle from the contralateral side, especially in the large lesions cortical damage extended to more lateral and ventral regions. We cannot determine to which degree cortico-cortical projections were compromised. However, this has no impact on our key results, namely that global motion perception is severely affected if present at all if lesions include area PSS. As this result is largely independent of the size of the lesion and the amount of white matter disruption our results indicate that area PSS is the key structure for the perception of global motion in the ferret. This holds true both for pigmented and albino ferrets therefore suggesting that motion discrimination is based on similar neural circuits and computations in both phenotypes.

In conclusion, our data show that ferret area PSS is crucially involved in global motion perception both in wildtype and albino animals. Area PSS is additionally involved in the cortical control of slow eye movements in wildtype ferrets but can not be held responsible for the loss of optokinetic reactions in albino ferrets. Thus, our findings strongly support the notion that ferret area PSS subserves functions similar to cat area PMLS and monkey area MT. Following the criteria of Payne (1993), namely an area's relative position on the cortex, its visual field representation, and its neuronal connections added to the functions of PSS described above we might even suggest that area PSS is a homolog to cat PMLS and monkey MT.

Acknowledgements We thank B. Krekelberg for creating the stimulus software "randomdots" and S. Krämer, H. Korbmacher, and S. Dobers for expert technical assistance. We are also grateful for the constructive comments of the anonymous reviewers which helped to improve earlier versions of the manuscript. This study was supported by DFG grant Sonderforschungsbereich 509.

References

Abadi RV, Pascal E (1994) Periodic alternating nystagmus in humans with albinism. Invest Ophthalmol Vis Sci 35:4080–4086

Albright TD, Desimone R, Gross CG (1984) Columnar organization of directionally selective cells in visual area MT of the macaque. J Neurophysiol 51:16–31

Baker GE, Thompson ID, Krug K, Smythe D, Tolhurst DJ (1998) Spatial-frequency tuning and geniculocortical projections in the visual cortex (areas 17 and 18) of the pigmented ferret. Eur J Neurosci 10:2657–2668

Beardsley SA, Vaina LM (2006) Global motion mechanisms compensate local motion deficits in a patient with a bilateral occipital lobe lesion. Exp Brain Res 173:724–732

Berson DM, Graybiel AM (1980) Some cortical and subcortical fiber projections to the accessory optic nuclei in the cat. Neuroscience 5:2203–2217

Blanke O, Landis T, Mermoud C, Spinelli L, Safran AB (2003) Direction-selective motion blindness after unilateral posterior brain damage. Eur J Neurosci 18:709–722

Brosseau-Lachaine O, Faubert J, Casanova C (2001) Functional sub-regions for optic flow processing in the posteromedial lateral suprasylvian cortex of the cat. Cereb Cortex 11:989–1001

Cantone G, Xiao J, Levitt JB (2006) Retinotopic organization of ferret suprasylvian cortex. Vis Neurosci 23:61–77

Collewijn H, Winterson BJ, Dubois MF (1978) Optokinetic eye movements in albino rabbits: inversion in anterior visual field. Science 199:1351–1353

Collewijn H, Apkarian P, Spekreijse H (1985) The oculomotor behaviour of human albinos. Brain 108:1–18

Demer JL, Zee DS (1984) Vestibulo-ocular and optokinetic deficits in albinos with congenital nystagmus. Invest Ophthalmol Vis Sci 25:739–745

Distler C, Mustari M, Hoffmann K-P (2002) Cortical projections to the nucleus of the optic tract and dorsal terminal nucleus and to the dorsolateral pontine nucleus in macaques: a dual retrograde tracing study. J Comp Neurol 444:144–158

Distler C, Korbmacher H, Hoffmann K-P (2006) Neuronal connections of motion sensitive area PSS of the ferret (*Mustela putorius furo*). FENS Forum Abstracts 3:A216.4

Duersteler MR, Wurtz RH (1988) Pursuit and optokinetic deficits following chemical lesions of cortical areas MT and MST. J Neurophysiol 60:940–965

Fox JG (1998) Biology and diseases of the ferret. Lippincott Williams and Wilkins, Philadelphia

Gallyas F (1979) Silver staining of myelin by means of physical development. Neurol Res 1:203–209

Guo K, Benson PJ, Blakemore C (1998) Residual motion discrimination using colour information without primary visual cortex. Neuroreport 9:2103–2107

Hahnenberger RW (1977) Differences in optokinetic nystagmus between albino and wildtype rabbits. Exp Eye Res 25:9–17

Hein A, Courjon JH, Flandrin JM, Arzi M (1990) Optokinetic nystagmus in the ferret: including selected comparisons with the cat. Exp Brain Res 79:623–632

Hess DT, Merker BH (1983) Technical modifications of Gallyas' silver stain for myelin. J Neurosci Methods 8:95–97

Hoffmann K-P, Garipis N, Distler C (2004) Optokinetic deficits in albino ferrets (*Mustela putorius furo*): a behavioural and electrophysiological study. J Neurosci 24:4061–4069

Hupfeld D, Distler C, Hoffmann K-P (2006) Motion perception deficits in albino ferrets (*Mustela putorius furo*). Vision Res 46:2941–2948. doi 10.1016/j.visres.2006.02.020

Huxlin KR, Pasternak T (2004) Training-induced recovery of visual motion perception after extrastriate cortical damage in the adult cat. Cereb Cortex 14:81–90

Innocenti GM, Manger PR, Masiello I, Colin I, Tettoni L (2002) Architecture and callosal connections of visual areas 17, 18, 19 and 21 in the ferret (*Mustela putorius*). Cereb Cortex 12:411–422

Jeffery G (1997) The albino retina: an abnormality that provides insight into normal retinal development. Trends Neurosci 20:165–169

Kawamura S, Sprague JM, Niimi K (1974) Corticofugal projections from the visual cortices to the thalamus, pretectum and superior colliculus in the cat. J Comp Neurol 158:339–362

Komatsu H, Wurtz RH (1988) Relation of cortical areas MT and MST to pursuit eye movements. I. Localization and visual properties of neurons. J Neurophysiol 60:580–603

Lagae L, Raiguel S, Orban GA (1993) Speed and direction selectivity of macaque middle temporal neurons. J Neurophysiol 69:19–39

Lauwers K, Saunders R, Vogels R, Vandenbussche E, Orban GA (2000) Impairment in motion discrimination tasks is unrelated to amount of damage to superior temporal sulcus motion areas. J Comp Neurol 420:539–557

Li B, Li BW, Chen Y, Wang LH, Diao YC (2000) Response properties of PMLS and PLLS neurons to simulated optic flow patterns. Eur J Neurosci 12:1534–1544

Lomber SG, Cornwell P, Sun JS, MacNeil MA, Payne BR (1994) Reversible inactivation of visual processing operations in middle suprasylvian cortex of the behaving cat. Proc Natl Acad Sci USA 91:2999–3003

Lynch JC, McLaren JW (1983) Optokinetic nystagmus deficits following parieto-occipital cortex lesions in monkeys. Exp Brain Res 49:125–130

Manger PR, Kiper D, Masiello I, Murillo L, Tettoni L, Hunyadi Z, Innocenti GM (2002) The representation of the visual field in three extrastriate areas of the ferret (*Mustela putorius*) and the relationship of retinotopy and field boundaries to callosal connectivity. Cereb Cortex 12:423–437

Manger PR, Masiello I, Innocenti GM (2002) Areal organization of the posterior parietal cortex of the ferret *(Mustela putorius*). Cereb Cortex 12:1280–1297

Manger PR, Nakamura1 H, Valentiniene S, Innocenti GM (2004) Visual areas in the lateral temporal cortex of the ferret (*Mustela putorius*). Cereb Cortex 14:676–689

Marcotte RR, Updyke BV (1982) Cortical visual areas of the cat project differentially onto the nuclei of the accessory optic system. Brain Res 242:205–217

Maunsell JH, Van Essen DC (1983) Functional properties of neurons in middle temporal visual area of the macaque monkey. I. Selectivity for stimulus direction, speed, and orientation. J Neurophysiol 49:1127–1147

Maunsell JH, Van Essen DC (1983) The connections of the middle temporal visual area (MT) and their relationship to a cortical hierarchy in the macaque monkey. J Neurosci 3:2563–2586

Moore BD, Alitto HJ, Usrey WM (2005) Orientation tuning, but not direction selectivity, is invariant to temporal frequency in primary visual cortex. J Neurophysiol 94:1336–1345

Nakamura H, Kashii S, Nagamine T, Matsui Y, Hashimoto T, Honda Y, Shibasaki H (2003) Human V5 demonstrated by magnetoencephalography using random dot kinematograms of different coherence levels. Neurosci Res 46:423–433

Newsome WT, Paré EB (1988) A selective impairment of motion perception following lesions of the middle temporal visual area (MT). J Neurosci 8:2201–2211

Newsome WT, Wurtz RH, Duersteler MR, Mikami A (1985) Deficits in visual motion processing following ibotenic acid lesions of the middle temporal visual area of the macaque monkey. J Neurosci 5:825–840

Nguyen AP, Spetch ML, Crowder NA, Winship IR, Hurd PL, Jantzie LL, Wylie DR (2004) A dissociation of motion and spatial-pattern vision in the avian telencephalon: implications for the evolution of "visual streams". J Neurosci 24:4962–4970

Palmer SM, Rosa MGP (2006) A distinct anatomical network of cortical areas for analysis of motion in far peripheral vision. Eur J Neurosci 24:2389–2405

Pasternak T, Merigan WH (1994) Motion perception following lesions of the superior temporal sulcus in the monkey. Cereb Cortex 4:247–259

Pasternak T, Tompkins J, Olson CR (1995) The role of striate cortex in visual function of the cat. J Neurosci 15:1940–1950

Payne BR (1993) Evidence for visual cortical area homologs in cat and macaque monkey. Cereb Cortex 3:1–25

Philipp R, Distler C, Hoffmann K-P (2006) A motion-sensitive area in ferret extrastriate visual cortex: an analysis in wildtype and albino animals. Cereb Cortex 16:779–790

Rauschecker JP, von Grunau MW, Poulin C (1987) Centrifugal organization of direction preferences in the cat's lateral suprasylvian visual cortex and its relation to flow field processing. J Neurosci 7:943–958

Rudolph KK, Pasternak T (1996) Lesions in cat lateral suprasylvian cortex affect the perception of complex motion. Cereb Cortex 6:814–822

Rudolph KK, Pasternak T (1999) Transient and permanent deficits in motion perception after lesions of cortical areas MT and MST in the macaque monkey. Cereb Cortex 9:90–100

Schenk T, Zihl J (1997) Visual motion perception after brain damage: I. Deficits in global motion perception. Neuropsychologia 35:1289–1297

Schmidt KE, Castelo-Branco M, Goebel R, Payne BR, Lomber SG, Galuske RAW (2006) Pattern motion selectivity in population responses of area 18. Eur J Neurosci 24:2363–2374

Sherk H (1988) Retinotopic order and functional organization in a region of suprasylvian visual cortex, the Clare-Bishop area. In: Hicks TP, Benedek G (eds) Progress in brain research, vol. 75: vision within extrageniculostriate systems, Elsevier, Amsterdam, pp 237–244

Sherk H, Fowler GA (2002) Lesions of extrastriate cortex and consequences for visual guidance during locomotion. Exp Brain Res 144:159–171

Spear PD, Baumann TP (1975) Receptive field characteristics of single neurons in lateral suprasylvian visual area of the cat. J Neurophysiol 38:1403–1420

Spear PD, Miller S, Ohman L (1983) Effects of lateral suprasylvian visual cortex lesions on visual localization, discrimination, and attention in cats. Behav Brain Res 10:339–359

Standage GP, Benevento LA (1983) The organization of connections between the pulvinar and visual area MT in the macaque monkey. Brain Res 262:288–294

St John RS, Fisk JD, Timney B, Goodale MA (1984) Eye movements of human albinos. Am J Optom Physiol Opt 61:377–385

Strong NP, Malach R, Lee P, Van Sluyters RC (1984) Horizontal optokinetic nystagmus in the cat: recovery from cortical lesions. Brain Res 315:179–92

Toyama K, Mizobe K, Akase E, Kaihara T (1994) Neuronal responsiveness in areas 19 and 21a, and the posteromedial lateral suprasylvian cortex of the cat. Exp Brain Res 99:289–301

Tusa RJ, Demer JL, Herdman SJ (1989) Cortical areas involved in OKN and VOR in cats: cortical lesions. J Neurosci 9:1163–1178

Ungerleider LG, Desimone R, Galkin TW, Mishkin M (1984) Subcortical projections of area MT in macaques. J Comp Neurol 223:368–386

Vaina LM, Soloviev S, Bienfang DC, Cowey A (2000) A lesion of cortical area V2 selectively impairs the perception of the direction of first-order visual motion. Neuroreport 11:1039–1044

Vaina LM, Cowey A, Jakab M, Kikinis R (2005) Deficits of motion integration and segregation in patients with unilateral extrastriate lesions. Brain 128:2134–2145

Ventre J (1985) Cortical control of oculomotor functions. I. Optokinetic nystagmus. Behav Brain Res 15:211–226

von Bonin G, Bailey P (1947) The neocortex of macaca mulatta. University of Illinois Press, Urbana

Zeki S (1991) Cerebral akinetopsia (visual motion blindness). A review. Brain 114:811–824